Role of phosphoric acid on the corrosion performance of Pb-1.7%Sb grid of lead-acid batteries

H.A. Abd El-Rahman*, S.A. Salih and A. A. Mokhtar
Chemistry Department, Faculty of Science, Cairo University, 12613 Giza, EGYPT.

Influencia del ácido fosfórico en el comportamiento frente a la corrosión de la malla de Pb-1,7%Sb en baterías de plomo-ácido

Influència de l'àcid fosfòric en el comportament enfront de la corrosió de la malla de Pb-1,7%Sb en bateries de plom-àcid

Recibido: 4 de agosto de 2011; revisado: 16 de noviembre de 2011; aceptado: 11 de enero de 2012

RESUMEN

El comportamiento frente a la corrosión de una malla comercial de Pb - 1,7% Sb en baterías de plomo-ácido en condiciones de circuito abierto en H_2SO_4 5M y en presencia de ácido fosfórico, se ha estudiado por espectroscopia de impedancia electroquímica y voltamperometría cíclica. La dependencia de la corrosión de la aleación de la concentración de H_3PO_4 es débil hasta 0.7M. Después de días de corrosión, la velocidad de corrosión en presencia de H_3PO_4 es ligeramente más alta que en su ausencia, debido al retraso en el crecimiento de un capa aislante de $PbSO_4$ que actúa como una barrera eficaz para la difusión de la especie corrosive. Las propiedades electrónicas y de difusión de la capa pasiva formada en presencia de H_3PO_4 son substancialmente inferiores. La voltametría cíclica indica una disminución en las cantidades de $PbSO_4$ y Sb_2O_3 formadas en presencia de concentraciones crecientes de H_3PO_4. Asimismo, la cantidad de PbO formada debajo de la capa de $PbSO_4$ crece con el aumento de la concentración de H_3PO_4 a expensas de la cantidad de $PbSO_4$.

Palabras clave: aleación plomo-antimonio; celda plomo-ácido; ácido fosfórico; corrosión ácida.

SUMMARY

The corrosion behavior of a commercial Pb-1.7%Sb grid of lead-acid batteries under open circuit conditions in 5 M H_2SO_4 in the presence of phosphoric acid is studied by electrochemical impedance spectroscopy and cyclic voltammetry. Dependence of corrodibility of the alloy on H_3PO_4 concentration is weak up to 0.7M. After days of corrosion, the corrosion rate in the presence of H_3PO_4 is slightly higher than in its absence, due to retardation of the growth of an insulating $PbSO_4$ layer that acts as an effective diffusion barrier of the corrosive species. The electronic and diffusion properties of the passive layer formed in the presence of H_3PO_4 are substantially inferior. Cyclic voltammetry indicates a decrease in amounts of $PbSO_4$ and Sb_2O_3 formed in the presence of H_3PO_4 and with increasing its concentration. Also, the amount of PbO formed beneath the $PbSO_4$ layer increases with increasing H_3PO_4 concentration on the expense of the amount of $PbSO_4$.

Keywords: Lead-Antimony alloys; Lead-acid cell; Phosphoric acid; acid corrosion.

RESUM

El comportament enfront de la corrosió d'una malla comercial de Pb - 1,7% Sb en bateries de plom-àcid en condicions de circuit obert en H_2SO_4 5M i en presència d'àcid fosfòric, s'ha estudiat per espectroscòpia d'impedància electroquímica i voltamperometria cíclica. La dependència de la corrosió de l'aliatge de la concentració d'H_3PO_4 és feble fins a 0.7M. Després de dies de corrosió, la velocitat de corrosió en presència d' H_3PO_4 és lleugerament més alta que en la seva absència, a causa del retard en el creixement d'un capa aïllant de $PbSO_4$ que actua com una barrera eficaç per a la difusió de l'espècie corrosiva. Les propietats electròniques i de difusió de la capa passiva formada en presència d'H_3PO_4 son substancialment inferiors. La voltametría cíclica indica una disminució en les quantitats de $PbSO_4$ i Sb_2O_3 formades en presència de concentracions creixents d'H_3PO_4. Tanmateix, la quantitat de PbO formada sota la capa de $PbSO_4$ creix amb l'augment de la concentració d'H_3PO_4 a costa de la quantitat de $PbSO_4$.

Paraules clau: aliatge plom-antimoni; cel·la plom-àcid; àcid fosfòric; corrosió àcida.

*Corresponding author: abdelrahman_hamid@hotmail.com; Tel: +202-35676565; Fax: +202-35685799

1. INTRODUCTION

Of all the extensive efforts to improve lead-acid batteries, inorganic additives to sulphuric acid electrolyte are less successful and most controversial. Boric acid was proposed as an additive with positive effects [1-3]. Other electrolyte additives include metal ions [4-14] and organics [15,16]. However, phosphoric acid is by far the most widely studied additive for commercial uses to improve the Pb-acid battery performance [17-38]. H_3PO_4 addition was found to reduce the sulfation, especially after deep discharge [17, 23-26], increase the cycle life [17, 23, 24,31] and slowing down the discharge [30]. The serious disadvantage of addition of H_3PO_4 was found to be a loss in cell capacity [27]. In a study by Meissner [34], the loss in capacity was found to decrease as the discharge rate increased. There are conflicting reports on the effect of addition of H_3PO_4 on the formation of PbO_2. Some reports have claimed improvement of PbO_2 formation [28,29] while others have found the opposite [21,23,27,30,38]. The presence of H_3PO_4 was found to increase the overpotential of both hydrogen and oxygen evolution reactions [30,32,33]. The effect of binary additives, such as phosphoric and boric acids, on the corrosion of the negative and the positive grids of a lead-acid battery were studied, and the results were explained in terms of H^+ ion transport and the morphological change of the $PbSO_4$ layer [38]. For Pb-Sb alloys, H_3PO_4 was found to decrease the negative effect of antimony in lead alloy [32].

The aim of the present work is to study the effect of H_3PO_4 on the corrosion of the grids of wet lead-acid batteries made of a commercial Pb-1.7%Sb alloy using impedance spectroscopy and cyclic voltammetry.

2. EXPERIMENTAL

The disc working electrodes were cut from rods of a commercial low-antimony cast alloy (nominal composition Pb-1.7%Sb). The cross sectional area of 0.11 cm2 was only left to contact the test solution. The alloy is currently used in manufacturing the grids of wet lead-acid car batteries to hold the active paste materials and it is supplied by Chloride, Egypt for Batteries. The alloy has the following chemical composition: 97.68% Pb, 1.697% Sb, 0.149% As, 0.014% Se, 0.028% Cu, 0.013% Bi, 0.002% Ag. The electrodes were mechanically polished with successive grades of emery papers up to 1200 grit, then washed with acetone, double distilled water and finally with a fine tissue so that the surface appeared bright and free from defect. Chemically ultra-pure sulphuric acid 98% and phosphoric acid 85% stocks were used for preparation of solutions by appropriate dilution using a doubly distilled water.

Measurements were conducted in unstirred naturally aerated 5 M H_2SO_4 acid solutions in the absence and the presence of phosphoric acid (0.1M – 1.0M) at a constant temperature of 25± 0.2°C. The different electrochemical measurements were carried using the electrochemical system IM6 Zahner electric, Meßtechink, Germany. The potential of the alloy electrode was measured versus a Hg/Hg2SO4/1MH2SO4 reference electrode (0.680V vs. SHE). Impedance measurements at a fixed frequency of 1.0 kHz were monitored using an ac potential of 3 mV peak to peak. The measurements revealed the impedance, Z (Ω), and the phase shift angle, q. The corresponding capacitance, C (F) and resistance, R (Ω) values were extracted from Z and q values. Impedance data were averaged automatically for 10 times before recording to improve the sensitivity. Impedance spectra were recorded at the corrosion potential in the frequency range 0.1 Hz - 100 kHz. The experimental impedance spectra were fitted with the appropriate equivalent circuits using the "SIM" program included with the IM6 package. SIM allows the construction of the equivalent circuits, performs the fitting of the experimental data and outputs the values of the elements involved in the equivalent circuit. The suitability of the elements in the proposed equivalent circuit was judged by the error% of the fitting and comparing the calculated and the experimental impedance plots.

3. RESULTS AND DISCUSSION

3.1. Effect of H_3PO_4 concentration:

Fig. 1 shows the quasi-steady corrosion potential, E_{corr}, Capacitance, C, and Resistance, R, of Pb-1.7% Sb alloy in 5 M H_2SO_4 containing H_3PO_4 of different concentrations. The values were recorded after 3 hours of corrosion. As can be seen, Ecorr decreases slightly as $[H_3PO_4]$ increases, ~ 7 mV per decade of concentration. E_{corr} values are close to the reversible electrode potential of the $Pb/PbSO_4$ couple in 5 M H_2SO_4 solution and hence the alloy surface is assumed to be covered with a passive layer of $PbSO_4$ [39,40]. Changes in C and R can be used cautiously to probe the insulating properties of the passive layer. C increases rapidly up to 0.2 M H_3PO_4 then it starts to decrease slightly with H_3PO_4 concentration. The initial increase in C is attributed to a decrease in thickness of the passive $PbSO_4$ layer on the alloy surface [39]. The slight decrease in C at $[H_3PO_4] > 0.2$ M may be attributed to a competitive deposition of a porous $PbHPO_4$ layer together with the $PbSO_4$ layer, not possible at low H_3PO_4 concentrations [36,37]. In agreement with C behavior, the change in R indicates a growth of an insulating layer at $[H_3PO_4] > 0.2$ M and a decrease in thickness of an insulating layer at $[H_3PO_4] < 0.2$ M.

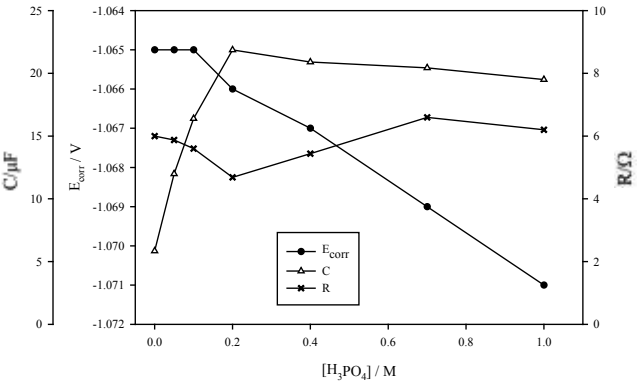

Fig. 1: *Steady corrosion potential, E_{corr}, Capacitance, C, and Resistance, R, of Pb-1.7% Sb alloy with H_3PO_4 concentration in 5 M H_2SO_4 containing H_3PO_4.*

Impedance spectra were recorded after 3 hours at the E_{corr} of Pb-1.7% Sb alloy in 5 M H_2SO_4 containing H_3PO_4 of different concentrations. The impedance data were simulated with several proposed equivalent circuits to account for the various processes involved at the alloy/solution

interface, beside the solution resistance. The proposed equivalent circuits (Models 1 and 2) are shown in Fig. 2. Model 1 consists of two parallel connections of resistive and capacitive elements for the passive film (R_1 and CPE_2), the faradaic processes (R_3 and W_4) and the double layer capacitance, Cdl, of the alloy/solution interface (CPE_5). The solution resistance, R_{sol} (element R_6) is added in series to the previously described parallel connections. R_1 and CPE_2 are identified as the film resistance, R_f and the film capacitance, C_f. Elements R_3 and W_4 are identified as the charge transfer resistance, R_{ct}, and the Warburg parameter, W, of the Warburg impedance, Z_W. Model 2 allows the nesting of the film properties in the traditional Randle's circuit of simple faradaic processes at metal/solution interface [41]. The constant phase elements, CPE_3 and CPE_5 are used instead of the conventional capacitances to account for the non-ideal capacitive behavior [42]. Each CPE is evaluated as a capacitance part and an exponential part, f. Other circuits without W or by replacing CPE with a conventional capacitance (i.e., with f = 1) were also examined. Fig. 3 shows the experimental and the simulated Bode plots with Models 1 and 2 for Pb-1.7%Sb alloy in 5 M H_2SO_4. Most results in the absence and the presence of H_3PO_4 were fairly fitted according to Model 2. The parameters used to fit Bode plots are shown in Fig. 4 in relation to phosphoric acid concentration.

As can be seen, R_{sol} values reflect relatively slight changes in solution resistances as a result of addition of various [H_3PO_4] to the more conductive 5 M H_2SO_4. R_{ct} represents the corrosion resistance of the alloy and it is slightly lower

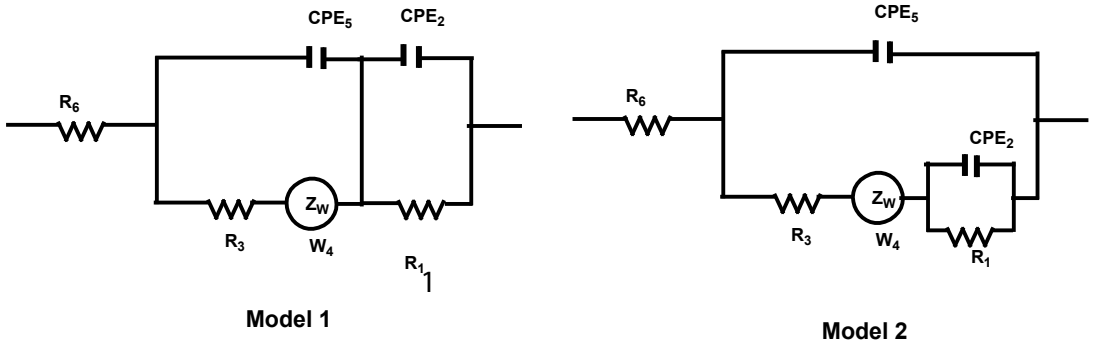

Fig. 2: *The equivalent circuits used to simulate the impedance data in the study.*

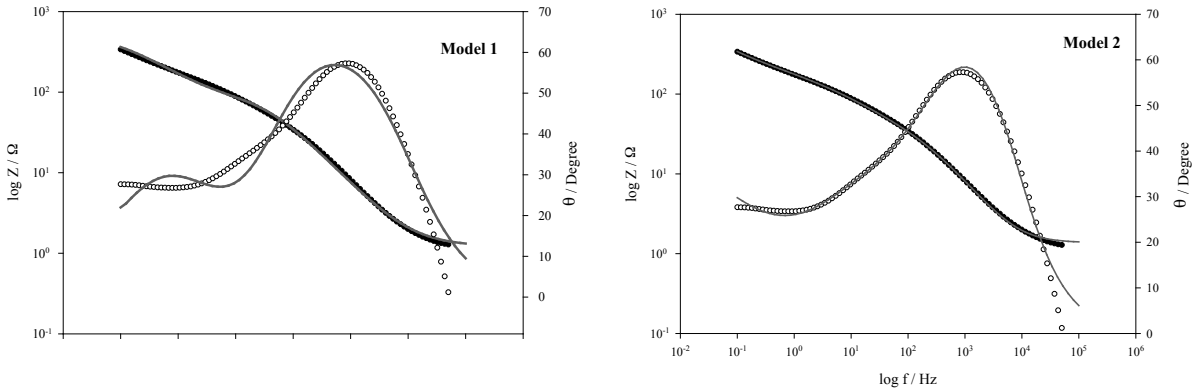

Fig. 3: *Simulation of Bode plots of Pb-1.7% Sb alloy in 5M H_2SO_4 at E_{corr} with different Models. Symbols) Experimental and Solid lines) Simulation.*

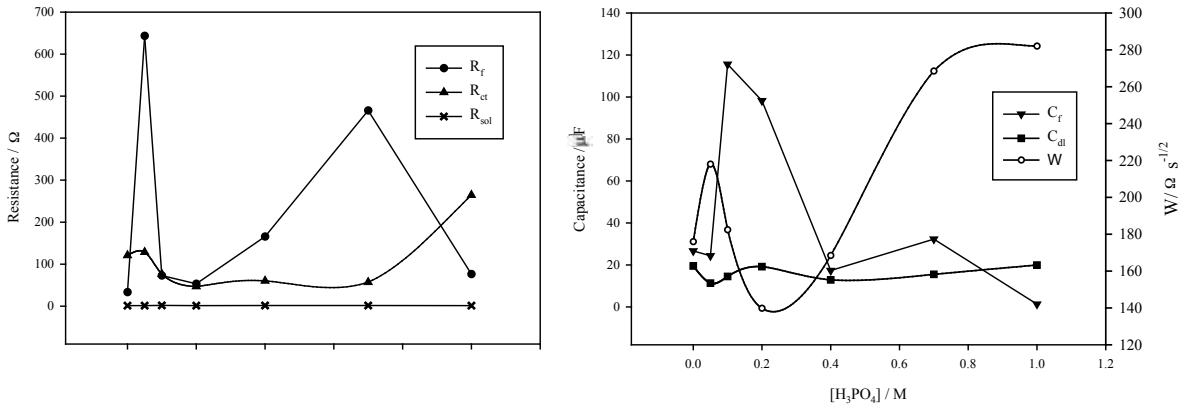

Fig. 4*: Dependence of fitting parameters of Bode plots on H_3PO_4 concentration.*

in the presence of H_3PO_4, except at $[H_3PO_4]$ = 1M. The decrease in R_{ct} in the presence of H_3PO_4 is consistent with a less effective (thinner) corrosion barrier as deduced from C and R behavior in Fig 1. The increase in R_{ct} in the presence of 1 M H_3PO_4 supports an improvement (thickening) of the corrosion barrier, probably by excessive deposition of $PbHPO_4$ beside $PbSO_4$. R_f is generally higher in the presence of H_3PO_4 and it shows a complex dependence on $[H_3PO_4]$. C_{dl} is practically independent on $[H_3PO_4]$. Both C_f and W show complex behaviors. At ³ 0.2M $[H_3PO_4]$, however, C_f sharply decreases with $[H_3PO_4]$ while W increases. This indicates substantial changes in the physical properties of the passive layer. Since W is inversely proportional to the diffusion coefficient(s) of the soluble species involved in corrosion of the alloy [41], one should deduce a decrease in the diffusion properties of the passive layer as $[H_3PO_4]$ increases, probably due to the presence of $PbHPO_4$ in the passive layer.

3.2. Effect of long corrosion time

Fig. 5 shows the variation of E_{corr}, C and R of Pb-1.7% Sb alloy with number of days of corrosion in 5 M H_2SO_4 in the absence and the presence of 0.4 M H_3PO_4. As can be seen, E_{corr} shifts in both solutions towards more positive potentials to reach a quasi-steady value of ~ -0.51 V after 4 days of corrosion. The presence of H_3PO_4 leads to retardation of the potential shift in the anodic direction so that no steady E_{corr} could be reached after 4 days of corrosion. The quasi-steady E_{corr} value in the absence of H_3PO_4 is close to the reversible potential of Sb/Sb_2O_3 electrode [39]. The electrode potential of Sb/Sb_2O_3 is -0.50 V in 5 M H_2SO_4 [40]. Previous studies on Pb-Sb alloys, with 1.5%-5.6% Sb, in 5 M H_2SO_4 have reported comparable E_{corr} values to these of the present study, and the anodic E_{corr} shift was attributed to the formation and growth of Sb_2O_3 [43]. The formation of PbO, with a reversible electrode potential of -0.426V in 5 M H_2SO_4 is assumed improbable. The reason for the induction period of several days before the formation of Sb_2O_3 seems to be related to nature and thickness of the $PbSO_4$ layer from one hand and the solubility of Sb_2O_3 in acidic solutions from the other hand. As the thickness of $PbSO_4$ layer increases a local environment beneath the layer, with less acidity, is formed and Sb2O3 can survive the acid attack and dissolution according to:

$$Sb_2O_3 + 2H^+ \rightarrow 2SbO+ + H_2O \qquad (1)$$

The results indicate that H_3PO_4 delays the Sb_2O_3 formation, most probably, by impeding the growth of the passive $PbSO_4$ layer. C and R behaviors shown in Fig. 6 support this opinion; where C decreases with time while R increases, in a clear indication of growth of the insulating passive $PbSO_4$ layer. At one and the same corrosion time, One can see the large difference in C or R between H_3PO_4–free and H_3PO_4–containing solutions, and a strong retardation of growth of $PbSO_4$ layer in the presence of H_3PO_4 is easy to deduce. The presence of H_3PO_4 is associated with higher C and lower R, i.e. a thinner insulating layer composed of $PbSO_4$ and Sb_2O_3. Impedance spectra after different corrosion days in the absence and the presence of 0.4 M H_3PO_4 were recorded and fairly simulated with Model 2. Fig. 6 shows Bode plots recorded after 1 and 4 days of corrosion in the absence and the presence of 0.4 M H_3PO_4. The corresponding simulated Bode plots are also shown in the figures. As can be seen, Bode plots change significantly with time and with addition of H_3PO_4. The large increase in the impedance value with time is an indication of the thickening of the insulating layer formed on the alloy surface. At intermediate frequencies, nearly linear log Z – log f portions could be distinguished, with slope values (dZ/dlog f) of -0.5 and -0.6 in the absence and presence of H_3PO_4, respectively. These slope values indicate ideal and non-ideal diffusion controls in the absence and the presence of H_3PO_4, respectively [41].

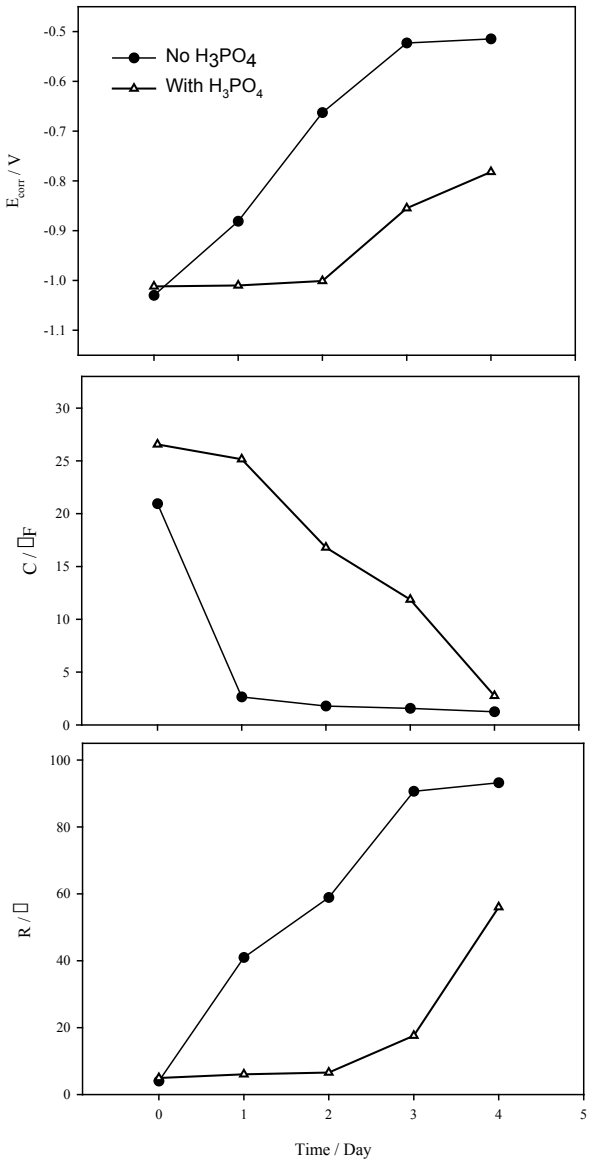

Fig. 5: *Variation of corrosion potential, E_{corr}, capacitance, C, and resistance, R, of Pb-1.7% Sb alloy with time in 5 M H_2SO_4 in the absence and the presence of 0.4 M H_3PO_4.*

Dependence of some parameters used to fit Bode plots shown in Fig. 6 on corrosion time is shown in Fig. 7. Rf in the absence of H_3PO_4 is about 3 orders of magnitude higher than in the presence of H_3PO_4, in a clear support of the previously discussed E_{corr}, C and R data and a strong indication of better insulating properties of the corrosion product layer formed in the absence of H_3PO_4. Also, Rct in the absence of H_3PO_4 is higher, i.e. corrosion rate is lower, though the difference narrows as corrosion time increases. The maximum Rct in the absence of H_3PO_4 is reached after 2 days but could not be reached in the presence of H_3PO_4 even after 4 days. The delaying effect H_3PO_4 is also

reflected in CdI values. The CdI values in the absence of H_3PO_4 are lower than in its presence but the difference narrows with time. Cf values in both solutions run almost parallel, with higher Cf values in the absence of H_3PO_4, though they become comparable after 4 days. It is interesting to see that the difference between the resistive properties of the passive layer (Rf values) in the absence and the presence of H_3PO_4 is huge, while the difference in the dielectric properties (Cf values) is slight. This may signify a compositional change of the passive layer in H_3PO_4-containing solutions, probably as mentioned before, via deposition of $PbHPO_4$ together with $PbSO_4$ and Sb_2O_3.

The most pronounced effect of addition of 0.4 M H_3PO_4 to 5 M H_2SO_4 on long period corrosion is reflected on the Warburg parameter, W. While W values after 3 hours corrosion in the absence and the presence of H_3PO_4 are comparable, large differences between W values in H_3PO_4-free and H_3PO_4-containing solutions after corrosion for several days are seen. After days of corrosion W becomes in the order of tens of $k\Omega\ s^{-1/2}$ in H_3PO_4–free solution, but with addition of H_3PO_4 W decreases significantly to several $\Omega\ s^{-1/2}$ or much less. Thus, Warburg (diffusion) impedance decreases significantly in the presence of H_3PO_4. In other words, the diffusion coefficients of species involved in corrosion of alloy in the H_3PO_4-free solution are much lower than that in the H_3PO_4-containing solution. This can be understood when we consider that corrosion occurs via mass transfer of the corrosive and the corroding soluble species through the passive layer on the alloy surface. In H_2SO_4 alone the passive film is more protective, i.e. it retards effectively the transfer of soluble species, while in the presence of H_3PO_4 the passive film is less protective, i.e. it allows an easy transfer of soluble species.

3.3. Cyclic voltammetry

Fig. 8 shows ten consecutive cyclic voltammograms (CV's) for the oxidation of Pb-1.7%Sb alloy in 5 M H_2SO_4 at a scan rate of 50 mV s^{-1}. Peak A1 at -1.0 V is typical for formation of $PbSO_4$ layer and shoulder A1' is attributed to the formation of basic lead sulphate [42,44-46]. Peak A2 at -0.4 V is close to the redox potential of the couple Sb/Sb_2O_3 and formation of Sb_2O_3 under a porous $PbSO_4$ and basic $PbSO_4$ layer is assumed. The reactivation peak A3 at ~ 1.87 V occurs in region of PbO_2 formation and O_2 evolution. A corresponding peak for reduction of PbO_2 cannot be detected with the high scan rate used (50 mV s^{-1}). Peaks C2 and C1 are due to the reduction of basic $PbSO_4$ and $PbSO_4$, respectively [42,44-46]. Starting from the 2nd cycle, repeating the potential scan has a slight effect on position and magnitude of the peaks and consequently, thickening of the solid oxidation product layer is limited. Addition of H_3PO_4 has a pronounced effect on the redox peaks, as can be seen in Fig. 9, and it can be summarized as follows:

- There is a large increase in magnitude of the reactivation peak A3 at $[H_3PO_4] > 0.2$ M.
- The shoulder A1' seems to disappear in the presence of H_3PO_4 (Part C in Fig. 9).

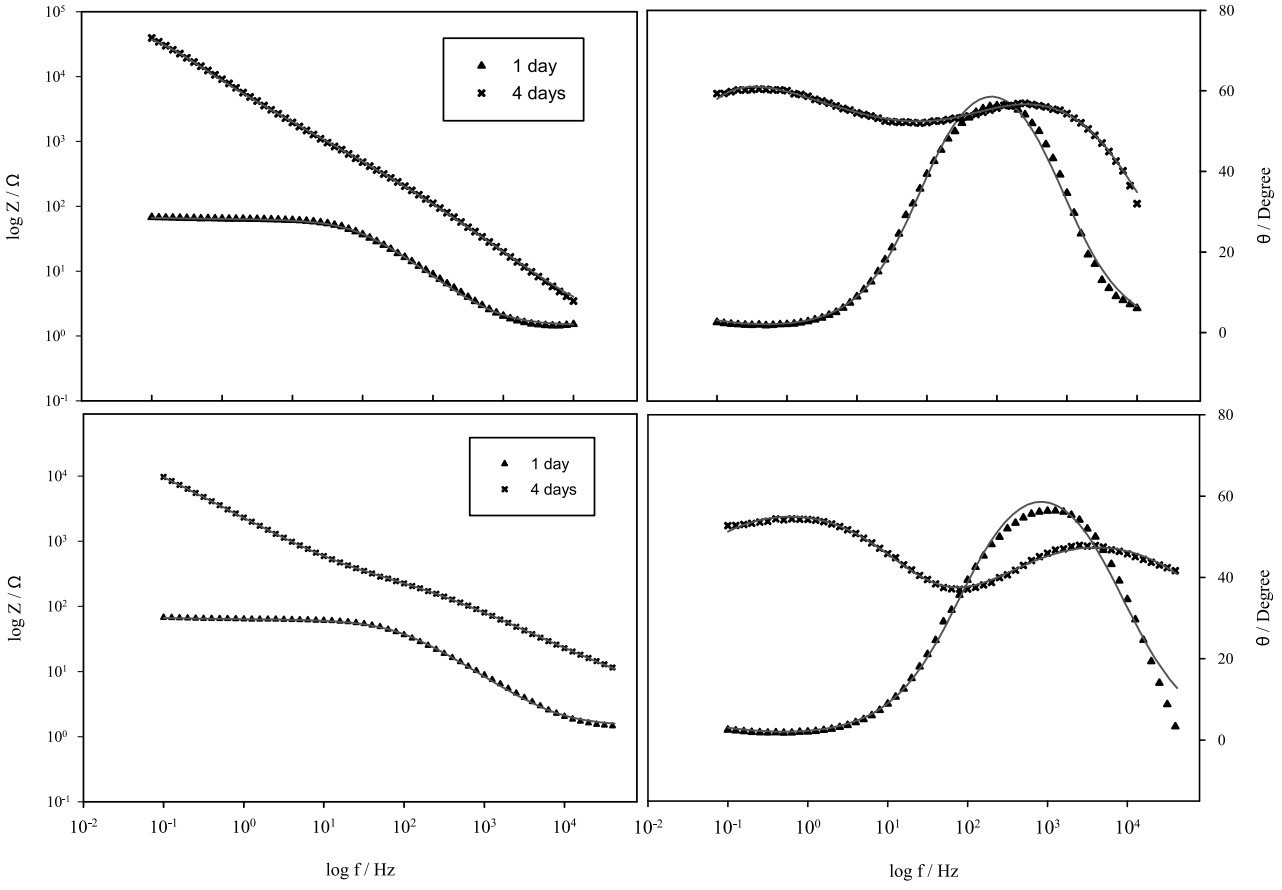

Fig. 6: *Bode plots of Pb-1.7% Sb alloy recorded after different corrosion times at E_{corr} in 5 M H_2SO_4 in the absence (Upper) and presence of 0.4M H_3PO_4 (Lower). Solid lines are the simulations using Model 2.*

- CV's do not show any oxidation peak (at ~ -0.6V) due to formation of $PbHPO_4$ [37].
- The presence of H_3PO_4 leads to a significant decrease in peak currents of peaks A1, A2 and C1 (Fig. 10), indicating the inhibitive action of H_3PO_4 toward the formation of both $PbSO_4$ and Sb_2SO_3
- In the presence of H_3PO_4, the reduction peak C2 shifts to more positive potentials (-0.94V) compare to that in the H_3PO_4–free solution (-1.01V) and its magnitude increases slightly with H_3PO_4 concentration. This may be explained by assuming the formation of small amounts of porous $PbHPO_4$ in the passive layer at high concentrations of H_3PO_4 [36,37]. The porosity of the passive layer at high concentrations of H_3PO_4 leads to an increase in the magnitude of the reactivation peak A3. The reduction of the insoluble Pb(II) species in both $PbHPO_4$ and basic $PbSO_4$ is assumed to be the reason of the positive shift of peak C2

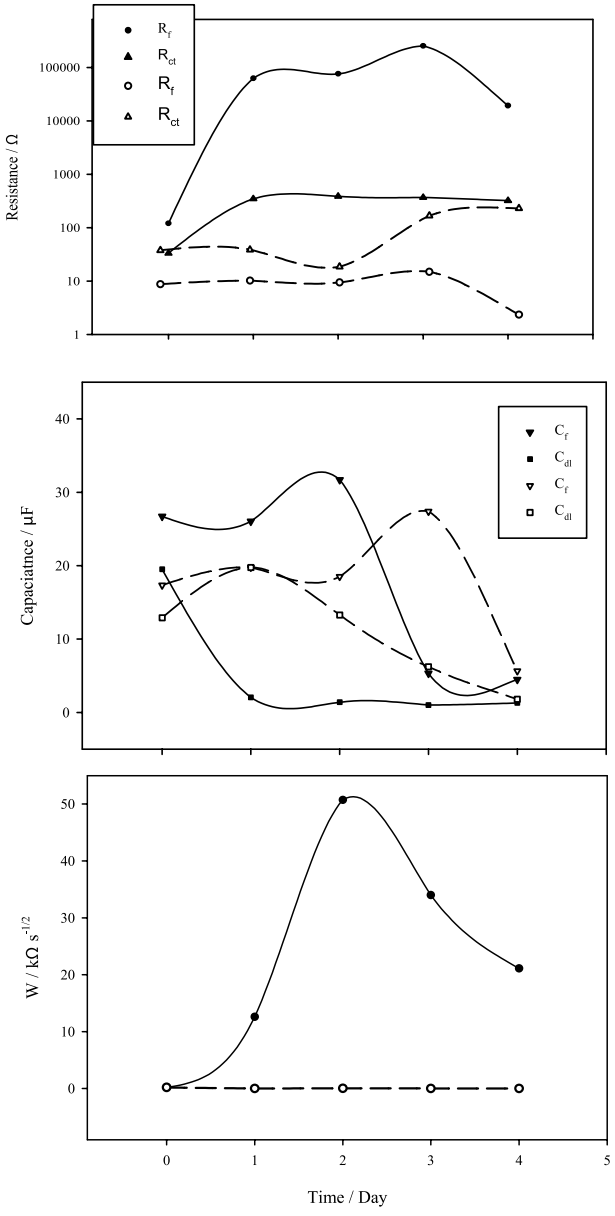

Fig. 7: *Dependence of fitting parameters of Bode plots on corrosion time in 5M H_2SO_4 in the absence (closed symbols, solid lines) and the presence of 0.4 M H_3PO_4 (opened symbols, dashed ines).*

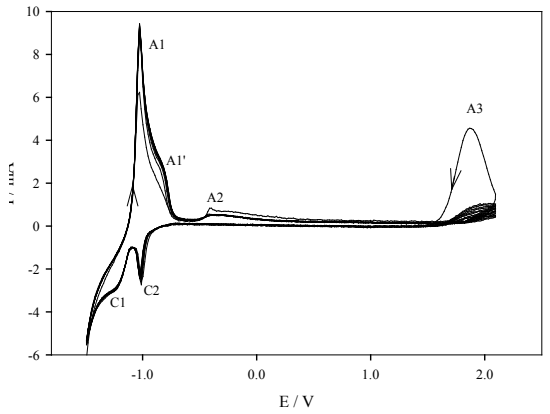

Fig. 8: *Ten consecutive cyclic voltammograms of Pb-1.7%Sb alloy in 5 M H_2SO_4 at a scan rate of 50 mVs^{-1}.*

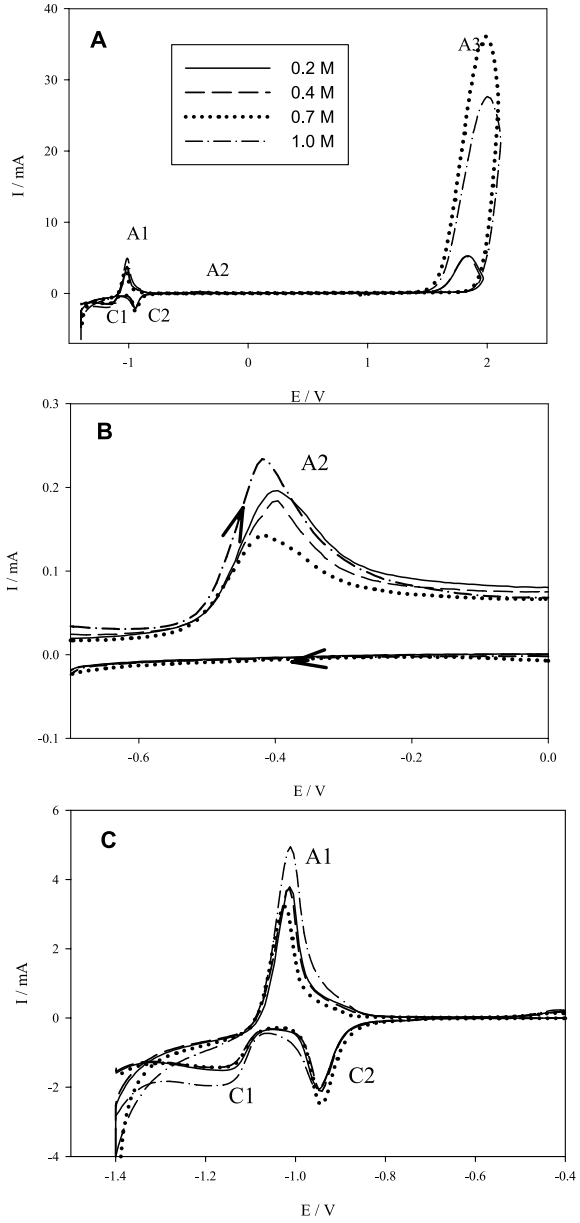

Fig. 9*: Cyclic voltammograms of Pb-1.7%Sb alloy in 5 M H_2SO_4 containing different concentrations of H_3PO_4 at a scan rate of 50 mV s^{-1}. Parts B & C are amplified Parts of the main voltammogram A.*

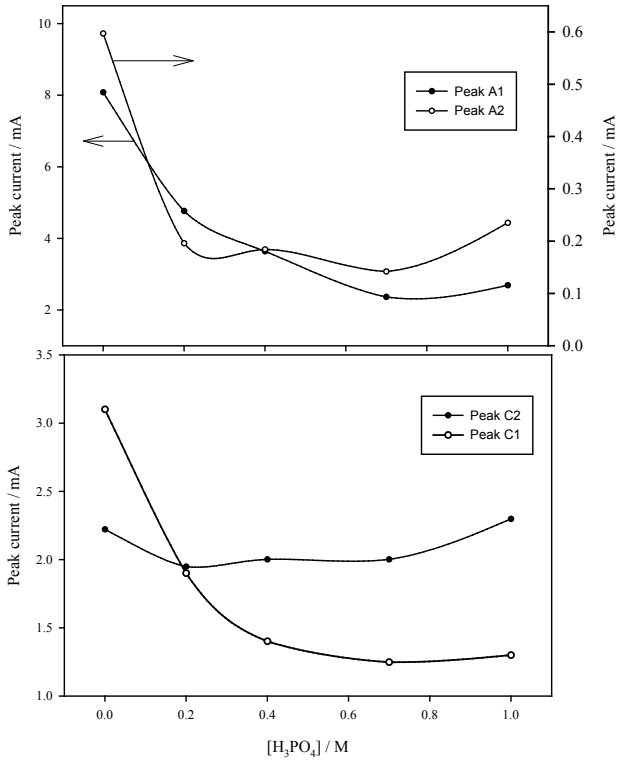

Fig. 10: *Peak currents versus H_3PO_4 concentration. Values were estimated from CVs in Fig. 9.*

4. CONCLUSION

The presence of H_3PO_4 up to 0.7M has a slight effect on the corrodibility after a few hours of corrosion while it has a pronounced effect on the composition of the passive $PbSO_4$ layer at concentrations > 0.2M.

The addition of 0.4 M H_3PO_4 leads, after a few days of corrosion, to a pronounced decrease in the passivation and insulating properties of the corrosion product layer via deposition of $PbHPO_4$ in the passive layer on the alloy surface, leading to delay of growth of the passive $PbSO_4$ layer. The apparent diffusion coefficients of the soluble species involved in controlling the corrosion rate increase in the presence of H_3PO_4 and consequently corrodibility of the alloy increases.

Addition of H_3PO_4 to 5 M H_2SO_4 solutions inhibits the formation of both $PbSO_4$ and Sb_2O_3 on Pb-1.7%Sb alloy, and leads to formation of small amounts of $PbHPO_4$ that change the composition and properties of the passive layer.

5. BIBLIOGRAPHY

1. I.M. Ismail, A.H. El Abd, Chem. Age India, 34 (1983) 393.
2. Yu.A. Zinchenko, O.L. Aleksandrova, M.R. Biegul, A.1. Petrukhova and V.D. Bar'Sukov, Tovarnye Znaki 48 (1971) 1194.
3. W.A. Badawy, S.S. El-Egamy, J. Power Sources 55 (1995) 11-17
4. B.K. Mahato, W.H. Tiedemann, J. Electrochem. Soc. 130 (1983) 2139.
5. L.T. Lam, J.D. Douglas, R. Pilling, D.A.J. Rand, J. Power Sources 48 (1994) 219.
6. H. Sanchez, Y. Meas, I. Gonzalez, M.A. Quiroz, J. Power Sources 32 (1990) 43.
7. M. Maja, N. Penazzi, J. Power Sources 22 (1988) 1.
8. K. Mc Gregor, J. Power Sources 59 (1996) 31.
9. D. Pavlov, J. Power Sources 33 (1991) 221.
10. D. Pavlov, A. Dakhouche, T. Rogachev, J. Power Sources 42 (1993) 71.
11. D. Pavlov, J. Power Sources 46 (1993) 171.
12. T. Rogachev, D. Pavlov, J. of Power Sources 64 (1997) 51-56
13. [N. Chahmanaa, M. Matrakovab, L. Zerroual, D. Pavlov, J. Power Sources 191 (2009) 51–57.
14. N. Chahmana, L. Zerroual, M. Matrakova, J. Power Sources 191 (2009) 144–148.
15. L. Torcheux, C. Rouvet, J.P. Vaurijoux, J. Power Sources 78 (1999) 147–155.
16. M. Ghaemi, E. Ghafouri, J. Neshati, J. Power Sources 157 (2006) 550–562.
17. S. Tudor, A. Weisstuch, S.H. Davang, Electrochem. Technol. 5 (1967) 21.
18. J. Burbank, J. Electrochem. Soc. 111 (1964) 1112.
19. B.K. Mahato, J. Electrochem. Soc. 126 (1979) 369.
20. E. Voss, J. Power Sources, 24 (1988) 171.
21. H.A. Laitinen, N. Walkins, Anal. Chem. 47 (1975) 1353.
22. K.R. Bullock, J. Electrochem. Soc., 126 (1979) 1848.
23. S. Tudor, A. Weisstuch, S.H. Davang, Electrochem. Technol., 4 (1966) 406.
24. S. Tudor, A. Weisstuch, S.H. Davang, Electrochem. Technol., 3 (1965) 90.
25. K.R. Bullock, D.H. McClelland, J. Electrochem. Soc. 124 (1977) 1478.
26. K.R. Bullock, J. Electrochem. Soc. 126 (1979) 360.
27. S. Stemberg, A. Mateescu, V. Branzoi, L. Apateanu, Electrochim. Acta 32 (1987) 349.
28. W. Visscher, J. Power Sources, 1 (1976/77) 257.
29. H. Doring, K. Wiesener, J. Garche, PI. Fischer, J. Power Sources, 38 (1992) 261.
30. S. Sternberg, V. Branzoi, L. Apateanu, J. Power Sources, 30 (1990) 177.
31. J. Garche, H. Doring, K. Wiesener, J. Power Sources, 33 (1991) 213.
32. S. Venugopalan, J. Power Sources 46 (1993) 1.
33. S. Venugopalan, J. Power Sources 48 (1994) 371.
34. E. Meissner, J. Power Sources 67 (1997) 135-150.
35. A. Bhattacharya, I. N. Basumallick, J. Power Sources 113 (2003) 382-387.
36. I. Paleskaa, R. Pruszkowska-Drachala, J. Kotowskia, A. Dziudzia, J.D. Milewskic, M. Kopczykc, A. Czerwinskia, J. Power Sources 113 (2003) 308–317.
37. S. Li, H.Y. Chen, M.C. Tang, W.W. Wei, Z.W. Xia, Y.M. Wu, W.S. Li, X. Jiang, J. Power Sources 158 (2006) 914–919.
38. K. Saminathan, N. Jayaprakash, B. Rajeswari, T. Vasudevan, J. Power Sources, 160 (2006)1410-1413.
39. [A.G. Gad-Allah, H.A. Abd El-Rahman, S.A. Salih, M. Abd El-Galil, Thin Solid Films 213 (1992) 244-250.
40. A.G. Gad-Allah, H.A. Abd El-Rahman, S.A. Salih, M. Abd El-Galil, J Appl. Electrochem. 22 (1997) 571-756.
41. A.J. Bard L.R. Faulkner, Electrochemical Methods Fundamentals and Applications, 2nd Ed., Wiley, New York, 2001, pp. 368-387.
42. M. Metikos-Hukovic, R. Babic, S. Brinic, J. Power Sources 157 (2006) 563–570.
43. A.G. Gad-Allah, H.A. Abd El-Rahman, M. Abd El-Galil, A. Al-Nadim, Hungarian J. Industrial chem., 25 (1997) 195-201.

44. Q. Sun, Y. Guo, J. Electroanal. Chem. 493 (2000) 123–129.
45. [E.N. Codaro, J.R. Vilche, Electrochim. Acta, 42 (1997) 549-55; 979-984.
46. E. Rocca, J. Steinmetz, J. Electroanal. Chem., 543 (2003) 153-160.